Assessment of the remineralisation induced by contemporary ion-releasing materials in mineral-depleted dentine

Paula Maciel Pires[1,6], Andrei Cristian Ionescu[2], Maria Teresa Pérez-Gracia[3], Elena Vezzoli[4], Igor Paulino Mendes Soares[5], Eugenio Brambilla[2], Aline de Almeida Neves[1], Salvatore Sauro[6*]

[1]. Department of Pediatric Dentistry, Universidade Federal do Rio de Janeiro, Rio de Janeiro, BRAZIL.

[2]. Oral Microbiology and Biomaterials Laboratory, Department of Biomedical, Surgical and Dental Sciences, Università degli Studi di Milano, Milano, ITALY.

[3]. Microbiology, Departamento de Farmacia, Cardenal Herrera-CEU University, CEU Universities, Valencia, SPAIN.

[4]. Department of Biomedical Sciences for Health, Università degli Studi di Milano, Milano, ITALY.

[5]. Department of Dental Materials and Prosthodontics, São Paulo State University UNESP, School of Dentistry, Araraquara, BRAZIL.

[6]. Dental Biomaterials and Minimally Invasive Dentistry, Department of Dentistry, Cardenal Herrera-CEU University, CEU Universities, Valencia, SPAIN.

Keywords: Dental biomaterials; Dentine replacement materials; Ions-releasing materials; Remineralisation; Restorative dentistry

Short title: Dentin remineralisation induced by ion-releasing materials

***Corresponding author:**

Prof. Dr. Salvatore Sauro

ORCID: 0000-0002-2527-8776

Dental Biomaterials, Preventive & Minimally Invasive Dentistry

Departamento de Odontología - Facultad de Ciencias de la Salud

Universidad CEU-Cardenal Herrera

46115 - Alfara del Patriarca, Valencia, Spain

salvatore.sauro@uch.ceu.es

ABSTRACT

Objectives: Evaluate the ion-releasing materials' ability to remineralise bacteria-driven artificial caries lesions.

Materials and Methods: Standardised class I cavities were obtained in 60 extracted human molars. Specimens underwent a microbiological cariogenic protocol (28d) to generate artificial caries lesions, then were randomly divided into four restorative groups: Adhesive+composite (negative control); Glass ionomer cement (GIC); calcium silicate cement (MTA); resin-modified calcium silicate cement (RMTA). Microhardness analysis (ΔKHN) was performed on 40 specimens (10/group, t=30d, 45d, 60d in artificial saliva, AS). Micro-CT scans were acquired (3/group, t=0, 30d, 90d in AS). Confocal microscopy was employed for interfacial ultra-morphology analysis (2/group, t=0, 60d in AS). Additional specimens (n=13) were prepared and processed for scanning electron microscopy (SEM) and FTIR (n=3/group + control) to analyse the ability of the tested materials to induce apatite formation on totally demineralised dentine discs (60d in AS). Statistical analyses were performed with a significance level of 5%.

Results: Adhesive+composite specimens showed the lowest ΔKHN values and the presence of gaps at the interface when assessed through micro-CT even after storage. Conversely, all the tested ions-releasing materials presented an increase in ΔKHN after storage ($p<0.05$), while MTA best reduced the demineralised artificial carious lesions gap at the interface. MTA and RMTA also showed apatite deposition on totally demineralised dentine surfaces (SEM and FTIR).

Conclusions: All tested ion-releasing materials expressed mineral precipitation in demineralised dentine. Additionally, calcium silicate-based materials induced apatite precipitation and hardness recovery of artificial carious dentine lesions over time.

Clinical Relevance: Overall, the use of ions-releasing materials can recover carious dentine. MTA shows enhanced ability of nucleation/precipitation of hydroxyapatite compared to RMTA and GIC which are more applicable for preservation/bio-remineralisation of the caries-affected collagen.

Keywords: Dental biomaterials; Dentine replacement materials; Ions-releasing materials; Remineralisation; Restorative dentistry.

1. INTRODUCTION

Preservation of dental hard tissues (i.e. dentine and enamel) through minimally invasive clinical approaches should be prioritised in contemporary operative dentistry [1-3]. Furthermore, selective carious tissue removal should be mainly considered an operative option for cavity preparation, especially in deep lesions near the pulpal chamber [4,5]. Indeed, it is advised to remove caries-infected dentine entirely while preserving the affected dentine [6]. Such an approach reduces the risk of excessive tissue removal with consequent unnecessary pulp exposure in deep cavities [7]. It was seen that tissue preservation is indeed one of the main factors improving a restoration's longevity, provided that the restoration is able to seal the carious cavity adequately [8]. Nevertheless, conventional adhesive systems partially infiltrate this demineralised caries-affected substrate due to its unfavourable chemical-morphological characteristics [9,10]. The collagen fibrils not infiltrated by the adhesive system are the leading cause of the low bond strength of the whole composite restoration and its reduced longevity [2,11].

A reasonable approach to restoring caries-affected dentine is represented by the use of pulp-protective materials with high remineralisation properties [12,13]. However, in such a scenario, there is still a need to develop innovative restorative materials, which should possess adhesive properties and the ability to "repair" caries-affected tissues through ion-releasing remineralisation processes [2,14,15]. The research yielded several materials based on such repairing properties, each having pros and cons so that the ideal restorative material with remineralising properties is still missing. Among the materials available nowadays, glass-ionomer cements (GICs), calcium silicate-based cements, and resin-modified types of the latter are commonly employed as restorative materials after selective caries removal [2,16]. GICs were demonstrated to exhibit chemical adhesion to dental hard tissues thanks to a well-known ion exchange process [17,18]. Moreover, such materials are responsible for the long-term fluoride release in

the microenvironment [19]. The latter can prevent the formation of recurrent lesions along the margins of the restoration [8,20]. The resin-modified hydraulic calcium-silicate cement (resin-modified mineral trioxide aggregate, RMTA) showed sustained release of Ca^{2+} and OH^- ions [21], able to induce tissue remineralisation [22]. Moreover, RMTA is a photocuring material that can be relatively compatible with an adhesive restoration [23]. However, data comparing the remineralising abilities of such materials in conditions as similar as possible to the clinical ones are still scarce and inconsistent.

The purpose of this study was to investigate the remineralising effect of different ion-releasing restorative materials in mineral-depleted simulated carious dentine by means of microhardness test and micro-CT analysis. The tooth-material interface ultra-morphology was also analysed through confocal scanning microscopy (CLSM). Moreover, the ability of the tested materials to induce apatite precipitation in demineralised dentine was assessed through scanning electron microscopy (SEM) and Fourier transform infrared spectroscopy (FTIR). The null hypothesis was that the tested materials would be able to remineralise the affected dentine to the same extent.

2. MATERIALS AND METHODS

2.1. Specimen preparation

Sound human molars (n=73), extracted for periodontal or orthodontic reasons, were collected according to the guidelines of the local ethics committee, under protocol number (blind for revision) and stored in distilled water at 4 ˚C for no longer than 3 months. Figure 1 shows the distribution of the specimens based on the experimental groups and methodological procedures.

Standardised class I cavities (4 mm length × 3 mm width) were obtained in 60 teeth with the floor ending in deep dentine (4 mm deep), using a high-speed handpiece with a cylindrical diamond bur (3146, Komet, Germany). Subsequently, the roots were removed

1 mm below the cement–enamel junction using a diamond-embedded blade (XL 12205; Benetec, London, UK) mounted on a low-speed microtome (Remet evolution, REMET, Bologna, Italy) under water cooling. All surfaces of the teeth were covered with an acid-resistant varnish (Deliplus®, Mercadona, Valencia, Spain), leaving only the dentine of the cavity exposed to be submitted to the cariogenic protocol.

The roots of the remaining teeth (n=13) were removed 1 mm beneath the cement–enamel junction as described previously. A second parallel cut was made to remove the occlusal enamel. Mid-coronal dentine was exposed and flattened using 320-grit SiC papers. These specimens were stored at 4˚C and 100% humidity until further use.

2.2. Artificial caries lesions formation

The Class I cavity specimens were fixed on the bottom of 24-well polystyrene plates (TPP, Zellkultur Testplatte 24F, Trasadingen, Switzerland) and sterilised under UV light for 40 minutes before receiving the microbial inoculum, according to the methodology previously described by Pires et al., [24]. The following bacterial strains were obtained from the type culture collection (CECT, Paterna, Valencia, Spain) used to prepare the inoculum: *Streptococcus mutans* (CECT 479T), *Streptococcus gordonii* (CECT 804), *Streptococcus salivarius* (CECT 805T) and *Lactobacillus casei* (CECT 475T). A pure suspension of each microorganism was obtained in Brain Heart Infusion (BHI, used as nutrient growth substrate) after overnight incubation in a 5% supplemented CO_2 environment at 37 °C. Cells were harvested by centrifugation (2200 x g, 19°C, 5 min), washed twice with phosphate-buffered saline (PBS), and resuspended. The suspension was then subjected to low-intensity ultrasonic energy (Sonifier model B-150; Branson, Danbury, CT, USA) to disperse bacterial chains and was finally adjusted to an equivalent of 0.5 on the McFarland scale.

Twelve µL (1.5×10^8/well) of the microbial inoculum was placed in each well along with the brain-heart infusion (BHI) broth with 5 wt.% of sucrose. The plates were incubated at 37 °C in a 5% CO_2 supplemented atmosphere to allow biofilm growth. Every 24 h, the

growth medium in each well was replaced with a fresh one, and the pH was monitored (Sension+ PH3, HACH LANGE, Barcelona, Spain). There was also a control plate without microorganisms to assess possible issues related to contamination. After 28 days, the specimens were gently detached from the plates and biofilm was detached by immersion in an ultrasonic bath for 5 minutes. The specimens were then immersed in ethanol (97%) for 2 min and rinsed with PBS for 1 min.

2.3. Restorative procedures

Tooth specimens with artificial caries lesions were randomly allocated to four experimental groups (n = 15 / group) based on the tested restorative materials (Table 1). According to the manufacturer's instructions, each dental cavity was filled with one of the materials.

- GIC: Specimens were rinsed with tap water (20 s) and air-dried (5 s). The GIC (Fuji IX, GC, Japan) powder was divided into 2 equal parts: the first aliquot was mixed with the GIC liquid for 10 s while the remaining one was subsequently incorporated and mixed for the following 20 s (ratio powder / liquid 1:1). The material was finally applied into the cavities without pre-conditioning the dentine. The material was left to set for 10 min.

- MTA: Specimens were rinsed with tap water (20 s) and air-dried (5 s). The cement (Endo-Pass, DEI Italia, Italy) was mixed with bi-distilled water (powder / water ratio = 2:1) to obtain a creamy consistency. The cement was placed in the cavity and left to set in contact with a wet cotton pellet for 20 min.

- RMTA: Specimens were rinsed with tap water (20 s) and gently air-dried (5 s), leaving the dentine moist. The RMTA (TheraCal LC, Bisco Inc, USA) was placed in incremental layers of 1 mm without any previous dentine treatment. Each increment was light-cured for 20 s using an LED curing unit (Radii plus, SID Ltd., Bayswater VIC, Australia, 1200 mW/cm^2).

- Negative control: Specimens were rinsed with tap water (20 s) and air-dried (5 s). Then, a universal adhesive (ZipBond, SDI, Australia) was used in self-etch mode. The adhesive was brushed inside the cavity for 10 s using a microbrush, left for 10 s, air-blown for 5 s to evaporate the solvent, then light-cured using the LED light-source (Radii plus) for 10 s. The specimens were restored with a flowable resin composite (Aura, SDI, Australia), applied in 2 mm increment layers, each light-cured for 20 s (Radii plus).

All specimens were incubated at 37 ˚C in artificial saliva for 24 h before further processing. The composition of the AS was 0.103 g L^{-1} of $CaCl_2$, 0.019 g L^{-1} of $MgCl_2$ x $6H_2O$, 0.544 g L^{-1} of KH_2PO_4, 30 g L^{-1} of KCl, and 4.77 g L^{-1} HEPES (acid) buffer, pH 7.4 [25]. This solution was replaced with a fresh batch every 7 days throughout the experiment.

2.4. Microhardness evaluation

Specimens (n = 10 / group) were prepared for microhardness analysis. These were first embedded in epoxy resin and then cut into 1.5 mm slabs perpendicular to the occlusal surface to expose the tooth-material interface. Slices not containing a tooth-material interface were discarded. On each slice, three parallel indentation series were performed. In each series, the first probing (25 gf load; 30 s dwell time) was made 50 µm away from the interface, while additional three indentations were performed below the first one (throughout the artificial caries lesion) at 50 µm intervals (Figure 1). Each specimen was tested 24 h after restoration placement (baseline) and after storage in 25 ml of AS for 30, 45, and 60 days. The AS solution was replaced with a fresh one every 7 days.

The average microhardness was measured for each slab by an operator, who was unaware of the treatment groups. The percentage difference between each storage time-point with baseline was calculated for each group at different depths (ΔKHN%).

2.5. Micro-CT analysis

A total of 12 restored specimens (n=3/group) were scanned (Skyscan 1176, Bruker, Kontich, Belgium) 24h after restoration (t0) and after 30 and 90 days of storage at 37 °C in AS (t30 and t90, respectively). The acquisition parameters were: 80 kV, 300 µA source current, 8.92 µm isotropic pixel size, 0.5 mm Al + 0.38 mm Cu filter, 0.5° rotation step over 360° with frame averaging of 5. Reconstruction was performed using proprietary software (NRecon, Bruker) using standardised parameters of beam hardening correction (30%), smoothing = 7, smoothing kernel = 2 (Gaussian), ring artefact compensation = 20, and optimal contrast limits based on the initial scanning and reconstruction tests. Image data were then aligned and resliced using another proprietary software (Dataviewer v1.5.4.6, Bruker). After that, the volume (mm^3) of the demineralised dentine extending between the restoration and the sound tissue in each specimen and for each scanning time was obtained within the ImageJ platform (v1.8.0_112) by a single operator that was blinded regarding the experimental groups. The operator manually defined a visual region of interest (ROI) on each slice of the CT stacks. The presence of CT artefacts due to materials' radiopacity and air bubbles trapped inside materials during mixing procedures (especially GIC) prevented an automatic AI-based threshold detection method to be applied.

2.6. Confocal Microscopy – Interface analysis for mineral precipitation

Eight specimens (n = 2 / group) were prepared as previously described (Par. 2.4) and submitted to confocal microscopy to investigate the interfacial characteristics of the demineralised/remineralised dentine interfaces. After sectioning, half of the specimens were stored in AS for 60 days and the other half were immediately immersed in 0.5 wt% Xylenol Orange solution (XO: FITC – Merck Life Science SLU, Spain) for 24h at 37°C (pH: 7.2). XO is a calcium-chelator fluorophore commonly used as a dye to trace the deposition of minerals within the interfaces of restored teeth due to its ability to form complexes with Ca^{2+} ions [26]. Specimens stored in AS were immersed in XO solution

as the control specimens. After immersion in XO, all specimens were ultrasonicated for 2 min in an ultrasonic bath containing distilled water to remove excess XO and then polished for 30 s each side with 1200-grit and 2400-grit SiC papers. The specimens were finally ultrasonicated in distilled water for 5 min to remove the surface smear layer and immediately submitted to confocal microscopy analysis (CLSM - Olympus FV1000, Olympus Corp, Tokyo, Japan) a 63X/1.4 NA oil immersion lens and 514 nm LED illumination. Optical transmission and fluorescence (568 nm emission filter) images were obtained with a 1-µm z-step to optically section the specimens to a depth of up to 20 µm below the surface [27]. The z-axis scan of the interface surface was pseudo-coloured arbitrarily for improved visualisation and compiled into both single and topographic projections using the CLSM image-processing software (Fluoview Viewer, Olympus). The configuration of the system was standardised and used at constant settings for the entire investigation. Three to five image stacks were randomly captured and recorded, representing the most noteworthy morphological features observed along the dentine-material interfaces [28,29].

2.7. FTIR-ATR and FEG SEM – evaluation of mineral precipitation

Flat dentine specimens (n = 13) previously obtained (Par. 2.1) were divided into four groups (n = 3 / group, Figure 1) and demineralised in a 10% phosphoric acid solution for 48 h [28] except for one sound dentine specimen that was stored at 4º C and 100% humidity. The tested materials were placed in direct contact with the demineralised specimens as previously described. Orthodontic rubber bands were used to ensure tight contact between the material and dentine specimens. The chemical analysis was performed on the surfaces of the specimens before and after 60 days of AS storage in contact with the materials using an FTIR-ATR microspectroscopic system (Spectrum Two UATR; Perkin Elmer). Specimens were scanned (3,000 - 650 cm^{-1}) at a 4 cm^{-1} spectral resolution. For standardisation, an initial correction and normalisation were applied to all scans.

After that, the specimens were mounted on aluminium stubs, dehydrated in silica gel for 24 h, gold sputter-coated, and analysed using a field-emission gun scanning electron microscope (FEG-SEM S-4100; Hitachi, Wokingham, UK, acceleration voltage, 20 kV and 15-20 mm working distance) to observe the presence of mineral precipitation after storage in AS (t60) at different magnifications.

2.8. Statistical Analysis

Shapiro-Wilk's test was used to check the normality of distribution for all datasets (α=5%). Microhardness data (ΔKHN%) were first analysed using a three-way ANOVA model complemented with Sidak test considering the material type, the indentation depths, and the storage time-points as fixed factors (α=5%). Then, the Kruskal-Wallis/Dunn tests were used to compare the microhardness of materials within the same time-point, and Friedman tests compared the same material throughout the time-points (α=5%). These analyses were performed separately for each indentation depth or using the overall average of depths considering the interaction between the material type and the indentation depths ($p<0.001$). Regarding micro-CT data, homogeneity of variances was preliminarily assessed using Bartlett's test (α=5%) followed by two-way ANOVA analysis considering the material type and the scan time as fixed factors. Student's post-hoc t-test was used in consideration of the small number of specimens to assess significant differences between the groups (α=5%).

3. RESULTS

The results of the dentine microhardness assessment are depicted in Figure 2. When comparing the dentine microhardness using the overall average of depths, all ion-releasing materials provided a significant increase in microhardness when compared to the control group after 45 and 60 days ($p<0.05$). However, only MTA and RMTA induced an overall increase of the dentine microhardness at all the different storage time-points

(30, 45, and 60 days) ($p<0.05$; Figure 2A). Also, only the effect promoted by MTA on the overall dentine microhardness increased after 60 days compared with the other time-points ($p<0.05$).

Figure 2 B-D shows the dentine microhardness compared separately for each indentation depth. At 50 µm sampling (Figure 2B), all ion-releasing materials provided a significant increase in microhardness when compared to the control group at all time-points ($p<0.05$). However, only RMTA increased the dentine hardness after 60 days compared with the other time-points ($p<0.05$). At 100 µm sampling (Figure 2C), only MTA increased microhardness at all time-points ($p<0.05$). Also, only MTA and RMTA increased the microhardness over time ($p<0.05$; Figure 2C). There was no significant difference in dentine microhardness between groups at 150 µm and 200 µm depths over time (Figure 2D and 2E).

Shapiro-Wilk's test revealed that micro-CT data did not have normal distribution. Thus, a cubic root function transformation was applied to approach normality. A highly significant influence of both considered factors on demineralised volume can be seen, while no significant interaction between the factors was highlighted. The volume analysis shows a progressive decrease of the demineralised volume during storage. This decrease was significant for GIC and MTA at t90 compared to baseline (Figure 3). MTA produced the highest reduction in the demineralised volume, resulting in less than 50% of the carious volume after three months (t90). For RMTA, an initial, albeit non-significant reduction of volume was observed in t30, while no further reduction could be seen at t90. No volume reduction could be observed in the control group.

Confocal single projection images (Average Intensity Projection - AIP) of the specimens treated with the different materials and analysed at baseline and t60 are presented in Figure 4. At the baseline assessment, the calcium-staining dye highlighted the presence of an extended (100-120 µm) demineralised dentine layer just underneath the material-dentine interface in all tested materials (Figure 4A). At t60, the specimens restored with

the adhesive composite system (negative control) were still characterised by the presence of an extended layer of demineralised dentine with no sign of remineralisation and areas of possible collagen degradation (Figure 4B). Conversely, at t60 the specimens restored with GIC showed the presence of calcium-stained minerals at 20-30 µm depth underneath the GIC-dentine interface (Figure 4C). MTA specimens at t60 showed calcium-stained minerals accumulated only very few microns underneath the interface (Figure 4D). Similar to MTA, the RMTA specimens at t60 showed the presence of calcium-stained minerals that accumulated few microns underneath the RMTA-dentine interface (Figure 4E).

The SEM analysis confirmed the presence of demineralised dentine collagen in the negative control group at t60 (Figure 5A). Then again, no exposed collagen fibrils were observed at the dentine surface restored with GIC, but the presence of minerals on the top of the surface together with partially obliterated dentine tubules (Figure 5B). MTA specimens clearly showed needle-like crystals (Figure 5C), while RMTA showed globular-like crystals (Figure 5D) on the dentine surface. The difference in surface morphology of the deposits indicate that the mechanism of mineral recovery induced by these materials are indeed different.

The FTIR analysis (Figure 6) confirmed the presence of remineralised dentine in MTA and RMTA-treated specimens due to apatite deposition (CaP stretch vibrations at: 559 cm^{-1}, 598 cm^{-1}, 970 cm^{-1}, 1024 cm^{-1} 1088 cm^{-1}). GIC-treated specimens showed no apatite precipitation but the preservation of collagen phosphorylation (1030-1080 cm^{-1}) plus the presence of carbonates (870 cm^{-1}) corresponding to the v_2CO_3 vibrations. The same collagen phosphorylation (1030-1080 cm^{-1}) band could be observed in the demineralised dentine at baseline.

4. DISCUSSION

Understanding the bio-interaction at the interface between the tooth and ion-releasing materials is crucial in predicting the longevity of such restorations and their physicochemical properties [14,30]. The formulation of innovative adhesive systems and composites with ion-releasing properties [31,32] may represent an alternative to reduce the degradation and repair the resin-dentine interface through remineralisation [2,33]. Since “bioactive” materials release specific ions from their fillers, the exposed collagen fibrils inside the demineralised dentine would become filled with apatite crystals, so recovering the initial stiffness [34] and fossilising the endogenous proteases [35,36]. The results obtained with the GIC material showed an increase in microhardness over time in the demineralised dentine underneath the bonding interface to a maximum depth of 100 µm. However, at 50 µm depth, there was no significant difference compared to the negative control (composite) up to 45 days of AS storage. The micro-CT analysis only showed a slight reduction in demineralised volume. In a previous study of Pires et al. [31], the authors demonstrated through micro-CT analysis the potential of a GIC in increasing the mineral density of artificially-induced carious dentine, confirming our results.

Further confirmation of the remineralisation ability by the tested GIC was obtained using confocal microscopy. Indeed, a porous mineral accumulation was observed in demineralised dentine 30-40 µm underneath the GIC-dentine interface after 60 days of storage in AS. The SEM analysis showed the presence of mineral deposits on the demineralised dentine surface, while FTIR demonstrated that those deposits were not made by apatite. In accordance with these results, a study found that GICs may not be effective in remineralising simulated caries-affected dentine via intrafibrillar apatite deposition, even when analogues of salivary proteins were employed [37].

It is well known that GICs have the ability to undertake a dynamic ionic exchange with the surrounding microenvironment for a relatively long time [19,31,38,39]. Indeed, such materials exhibit chemical bonding to dental tissues, along with their ability to release

specific ions (e.g. fluoride, strontium) at the bonded interface, being classified as bioactive ion-releasing material [2,18,40].

The MTA and RMTA produced the highest increase in KHN values over time, especially at 50 and 100 µm underneath the interface. The micro-CT analysis confirmed the ability of MTA to reduce the demineralised volume significantly. Interestingly, this reduction did not occur to the same extent as RMTA, which showed a performance comparable to GIC. Confocal microscopy observations supported the difference in mineralisation ability of MTA and RMTA. MTA specimens showed only few microns of residual calcium-stained minerals, indicating that, after 60 days of storage, most of the caries-affected dentine was mineralised. On the contrary, RMTA-dentine interfaces were characterised by calcium-stained minerals accumulated 20-30 microns underneath the interface, indicating that such area was not yet wholly remineralised.

The results of this study agree with the literature that demonstrated dentine remineralisation in the presence of hydraulic calcium silicate cements [21,41]. Such studies demonstrated mineral precipitation with different shapes and dimensions in artificial carious dentine treated with a calcium silicate cement, but no evidence of collagen remineralisation. On the other hand, the RMTA material used in the present study is a light-cured resin-modified calcium silicate cement that can be considered a bioactive material [16,23,33], as confirmed by our results. In these MTA-based materials, an intrinsic instability and rearrangement of filler particles due to the release (or re-uptake) of ions are apparently not compatible with a material designed to be inert [39]. It can be speculated that the presence of a resin-based matrix, albeit hydrophilic, reduces the material's bioactivity once it is placed in the cavity. Therefore, since the bioactive materials tested in the present study showed different behaviour in remineralising artificial caries-affected dentine, the null hypothesis can be rejected.

When the universal adhesive and resin composite were used to restore the artificial caries-affected dentine substrate, an incomplete infiltration of the adhesive was

observed together with degradation over time. Furthermore, as shown by micro-CT and microhardness analyses, no sign of remineralisation and no significant increase in hardness was observed. Indeed, it is well known that the peculiar chemical and morphological characteristics of caries-affected dentine are mainly responsible for the unsatisfactory bonding performance of adhesive/composite restorations [42,43]. Moreover, the poorly resin-infiltrated dentine collagen fibrils underneath the resin–dentine interface are much more prone to collagen degradation due to hydrolytic and enzymatic activity [43,44].

Nevertheless, it has to be noted that the presence of a soft, caries-affected dentine layer at the bottom of a cavity does not affect a composite restoration's longevity, provided that good adhesion is obtained in the surrounding tissue to form a seal. In fact, such a condition can arrest the primary lesion progression [8].

The protocol used in this study to obtain artificial caries-affected lesions in class I cavities was suitable for creating an extended (100-120 µm) mineral-depleted dentine. Xylenol orange solution is a calcium-chelator fluorophore commonly used to trace the deposition of minerals within the interfaces of restored teeth due to its ability to form complexes with Ca^{2+} ions. Such a dye is able to bind dental substrates where there is a substantial availability of calcium-rich substrates expressing free ions, non-complexed calcium-based minerals, partially demineralised hydroxyapatite, or in case there is a freshly formed calcium-rich complex [26,45]. This latter aspect may support the speculation that the RMTA- or GIC-dentine interfaces induced less consistent and porous mineral precipitation underneath the interface. Conversely, the reason why the MTA-dentine interface showed only a slight signal was probably a consequence of increased mineralisation of the demineralised dentine, characterised by more complex calcium based-complex (e.g. hydroxyapatite, as supported by the results in SEM and FTIR analysis). This may also be the reason why the extended 100-150 µm mineral-depleted simulated caries dentine layer was not observed after prolonged storage of the

specimens treated with all the ion-releasing tested materials in AS. Moreover, due to their strongly alkaline pH, calcium silicate cements (MTA) have a caustic effect on demineralised collagen fibrils. The space left after their degradation is replaced by calcium carbonates and apatite-like minerals, which also penetrate several microns inside the dentine tubules [46,47].

The choice of bioactive dentine replacement materials often placed over caries-affected dentine has to be considered in the light of a minimally invasive tooth-restoration concept to preserve the substrate that is still remineralisable [4, 21]. Nevertheless, the behaviour of such materials has to be assessed in terms of translatability to the clinical setting when directly applied to caries-affected dentine. The interactions with overlying restorative materials and their influence on the mechanical performance of the whole restoration also have to be addressed. In this sense*, in vivo* comparative studies are needed to confirm their performance.

5. CONCLUSION

Contemporary ion-releasing materials such as GIC, MTA and RMTA can remineralise the artificial caries-affected dentine, but to different extents. MTA showed the highest ability to induce apatite precipitation and remineralisation of extended mineral-depleted dentine. Conversely, RMTA and GIC are probably more appropriate for preserving the demineralised collagen fibrils in the outer layer of caries-affected dentine and remineralising it.

6. COMPLIANCE WITH ETHICAL STANDARDS

Conflict of Interest: All authors gave their final approval and agreed to be accountable for all aspects of the work. They have no conflict of interest with respect to the authorship and/or publication of this paper.

Ethical approval: This article does not contain any studies with human participants or animals performed by any of the authors.

Informed consent: For this type of study, formal consent is not required. Human molars used in this study were collected according to the guidelines of the local Ethics Committee (CEI22/298).

Acknowledgement: Research facilities were supported by grants “Ministerio de Ciencia, Innovación y Universidades (PID2020-120346GB-I00) and Universidad CEU-Cardenal Herrera (Programa INDI 2021-2022)”(PI: SS). Paula Maciel Pires undertook a PhD exchange program at Cardenal Herrera University during part of the experimental assay and was supported by a CAPES grant from Brazil (grant numbers 88882.424807/2018-01 and 88881.188518/2018-01).

7. REFERENCES

1. Banerjee A (2013) Minimal intervention dentistry: part 7. Minimally invasive operative caries management: rationale and techniques. Br Dent J 21:107-111. doi:10.1038/sj.bdj.2013.106
2. Sauro S, Pashley DH (2016) Strategies to stabilise dentine-bonded interfaces through remineralising operative approaches: State of the art. Int J Adhes Adhes 69: 39-57. https://doi.org/10.1016/j.ijadhadh.2016.03.014
3. Schwendicke F, Frencken JE, Bjørndal L, et al (2016) Managing Carious Lesions: Consensus Recommendations on Carious Tissue Removal. Adv Dent Res 28:58-67. doi:10.1177/0022034516639271
4. Banerjee A, Frencken JE, Schwendicke F, Innes NPT (2017) Contemporary operative caries management: consensus recommendations on minimally invasive caries removal. Br Dent 223:215-222. https://doi.org/10.1038/sj.bdj.2017.672
5. Schwendicke F, Splieth C, Breschi L, Banerjee A, Fontana M, Paris S, Burrow MF, Crombie F, Page LF, Gaton-Hernandez P, et al (2019) When to intervene in the caries process? An expert Delphi consensus statement. Clin Oral Investig 23:3691–3703. https://doi.org/10.1007/s00784-019-03058-w
6. Banerjee A, Watson TF (2011) Pickard’s Manual of Operative Dentistry, ed 9. Oxford, Oxford University Press.
7. Pugach MK, Strother J, Darling CL, Fried D, Gansky SA, Marshall SJ, Marshall GW (2009) Dentin caries zones: mineral, structure, and properties. J Dent Res 88: 71–76. https://doi.org/10.1177/0022034508327552
8. Brambilla, E, & Ionescu, AC (2021) Oral Biofilms and Secondary Caries Formation. Oral Biofilms and Modern Dental Materials: Advances Toward Bioactivity.

9. Almahdy A, Downey FC, Sauro S, Cook RJ, Sherriff M, Richards D, Watson TF, Banerjee A, Festy F (2012) Microbiochemical analysis of carious dentine using Raman and fluorescence spectroscopy. Caries Res 46:432-40. doi: 10.1159/000339487
10. Zavgorodniy AV, Rohanizadeh R, Swain MV (2008) Ultrastructure of dentine carious lesions. Arch Oral Bio 53:124-32. doi: 10.1016/j.archoralbio.2007.08.007
11. Yoshiyama M, Doi J, Nishitani Y, Itota T, Tay FR, Carvalho RM,et al (2004) Bonding ability of adhesive resins to caries-affectedand caries-infected dentin. J Appl Oral Sci 12:171–6. https://doi.org/10.1590/s1678-77572004000300002
12. Hashem D, Mannocci F, Patel S, Manoharan A, Brown JE, Watson TF, Banerjee A (2015) Clinical and radiographic assessment of the efficacy of calcium silicate indirect pulp capping: a randomised controlled clinical trial. J Dent Res 94:562-8. doi: 10.1177/0022034515571415
13. Hashem D, Mannocci F, Patel S, Manoharan A, Watson TF, Banerjee A (2019) Evaluation of the efficacy of calcium silicate vs. glass ionomer cement indirect pulp capping and restoration assessment criteria: a randomised controlled clinical trial-2-year results. Clin Oral Investig 23:1931-1939. doi: 10.1007/s00784-018-2638-0
14. Giannini M, Sauro S (2021) “Bioactivity” in Restorative Dentistry: Standing for the Use of Innovative Materials to Improve the Longevity of Restorations in Routine Dental Practice. J Adhes Dent 7;23:176-178. doi: 10.3290/j.jad.b1179733
15. Carrilho M & D’Alpino PH (2018) Future perspectives for dental composites. In: Miletic V. Dental composite materials for direct restorations. Springer, pp 291-301
16. Sanz JL, Rodríguez-Lozano FJ, Llena C, Sauro S, Forner L (2019) Bioactivity of Bioceramic Materials Used in the Dentin-Pulp Complex Therapy: A Systematic Review. Materials (Basel) 12:1015. doi: 10.3390/ma12071015
17. Watson TF, Bartlett DW (1994) Adhesive systems: composites, dentine bonding agents and glass ionomers. Br Dent J 19;176:227-31. doi: 10.1038/sj.bdj.4808410
18. Van Meerbeek B, De Munck J, Yoshida Y, Inoue S, Vargas M, Vijay P, Van Landuyt K, Lambrechts P, Vanherle G (2003) Buonocore memorial lecture. Adhesion to enamel and dentin: current status and future challenges. Oper Dent 28:215-235.
19. Hahnel S, Ionescu AC, Cazzaniga G, Ottobelli M, & Brambilla E (2017) Biofilm formation and release of fluoride from dental restorative materials in relation to their surface properties. J Dent 60:14-24. https://doi.org/10.1016/j.jdent.2017.02.005
20. Wiegand A, Buchalla W, Attin, T (2007) Review on fluoride-releasing restorative materials—Fluoride release and uptake characteristics, antibacterial activity and influence on caries formation. Dent. Mater 23:343–362. https://doi.org/10.1016/j.dental.2006.01.022
21. Li X, De Munck J, Van Landuyt K, Pedano M, Chen Z, Van Meerbeek B (2017) How effectively do hydraulic calcium-silicate cements remineralise demineralised dentin. Dent Mater 33:434-445. doi: 10.1016/j.dental.2017.01.015
22. Lee BN, Lee BG, Chang HS, Hwang YC, Hwang IN, Oh WM (2017) Effects of a novel light-curable material on odontoblastic differentiation of human dental pulp cells. Int Endod J 50:464-471. https://doi.org/10.1111/iej.12642
23. Meraji N, Nekoofar MH, Yazdi KA, Sharifian MR, Fakhari N, Camilleri J (2018) Bonding to caries affected dentine. Dent Mater 34:236-245. doi: 10.1016/j.dental.2018.05.017
24. Pires PM, Santos TP, Fonseca-Goncalves A, Pithon MM, Lopes RT, Neves AA (2018) Mineral density in carious dentine after treatment with calcium silicates and polyacrylic acid based cements. Int Endod J 51: 1292-1300. https://doi.org/10.1111/iej.12941

25. Sauro S, Lin CY, Bikker FJ, Cama G, Dubruel P, Soria JM, D''Onofrio A, Gillam D (2016) Di-Calcium Phosphate and Phytosphingosine as an Innovative Acid-Resistant Treatment to Occlude Dentine Tubules. Caries Res 50:303-9. doi: 10.1159/000445444
26. Profeta AC, Mannocci F, Foxton R, Watson TF, Feitosa VP, De Carlo B, Mongiorgi R, Valdré G, Sauro S (2013) Experimental etch-and-rinse adhesives doped with bioactive calcium silicate-based micro-fillers to generate therapeutic resin-dentin interfaces. Dent Mater 29:729-41. doi: 10.1016/j.dental.2013.04.001
27. Sauro S, Watson T, Moscardó AP, Luzi A, Feitosa VP, Banerjee (2018) The effect of dentine pre-treatment using bioglass and/or polyacrylic acid on the interfacial characteristics foreskin-modified glass ionomer cements. J Dent 73:32–9. http://dx.doi.org/10.1016/j.jdent.2018.03.014
28. Tezvergil-Mutluay A, Seseogullari-Dirihan R, Feitosa VP, Cama G, Brauer DS, Sauro S (2017) Effects of Composites Containing Bioactive Glasses on Demineralised Dentin. J Dent Res 96:999-1005. doi: 10.1177/0022034517709464
29. Spagnuolo G, Pires PM, Calarco A, Peluso G, Banerjee A, Rengo S, Elias Boneta AR, Sauro S (2021) An in-vitro study investigating the effect of air-abrasion bioactive glasses on dental adhesion, cytotoxicity and odontogenic gene expression. Dent Mater 37:1734-1750. doi: 10.1016/j.dental.2021.09.004
30. Tahmasebi E, Alam M, Yazdanian M, Tebyanian H, Yazdanian A, Seifalian A, Mosaddad S (2020) Current biocompatible materials in oral regeneration: a comprehensive overview of composite materials. J Mater Res Technol 9. doi: 11731-11755. 10.1016/j.jmrt.2020.08.042
31. Pires PM, Neves AA, Makeeva IM, Schwendicke F, Faus-Matoses V, Yoshihara K, Banerjee A, Sauro S (2020) Contemporary restorative ion-releasing materials: current status, interfacial properties and operative approaches. Br Dent J 229:450-458. https://doi.org/10.1038/s41415-020-2169-3
32. Sauro S, Babbar A, Gharibi B, Feitosa VP, Carvalho RM, Azevedo Rodrigues LK, Banerjee A, Watson T (2018) Cellular differentiation, bioactive and mechanical properties of experimental light-curing pulp protection materials. Dent Mater 34:868-878. doi: 10.1016/j.dental.2018.02.008
33. Zafar MS, Amin F, Fareed MA, Ghabbani H, Riaz S, Khurshid Z, Kumar N (2020) Biomimetic Aspects of Restorative Dentistry Biomaterials. Biomimetics (Basel) 5:34. doi: 10.3390/biomimetics5030034
34. Babaie E, Bacino M, White J, Nurrohman H, Marshall GW, Saeki K, Habelitz S (2021) Polymer-Induced Liquid Precursor (PILP) remineralisation of artificial and natural dentin carious lesions evaluated by nanoindentation and microcomputed tomography. J Dent 109:103659. doi: 10.1016/j.jdent.2021.103659
35. Liu Y, Tjäderhane L, Breschi L, Mazzoni A, Li N, Mao J, Pashley DH, Tay FR (2011) Limitations in bonding to dentin and experimental strategies to prevent bond degradation. J Dent Res 90:953-68. doi: 10.1177/0022034510391799
36. Tjäderhane L, Nascimento FD, Breschi L, Mazzoni A, Tersariol IL, Geraldeli S, Tezvergil-Mutluay A, Carrilho MR, Carvalho RM, Tay FR, Pashley DH (2013) Optimising dentin bond durability: control of collagen degradation by matrix metalloproteinases and cysteine cathepsins. Dent Mater 29:116-135. https://doi.org/10.1016/j.dental.2012.08.004
37. Kim YK, Yiu CK, Kim JR, Gu L, Kim SK, Weller RN, Pashley DH, Tay FR (2010) Failure of a glass ionomer to remineralise apatite-depleted dentin. J Dent Res 89:230-5. doi: 10.1177/0022034509357172
38. Fathy SM. Remineralisation ability of two hydraulic calcium-silicate based dental pulp capping materials: Cell-independent model (2019) J Clin Exp Dent 11:360-366. doi: 10.4317/jced.55689

39. Daneshpoor N, Pishevar L (2020) Comparative evaluation of bioactive cements on biomimetic remineralisation of dentin. J Clin Exp Dent 12:291-299. doi: 10.4317/jced.56500
40. Owens B (2018) Bioactivity, Biocompatibility and Biomimetic Properties for Dental Materials: Clarifying the Confusion? Mod. App Dent Oral Health 2. doi: 10.32474/MADOHC.2018.02.000132
41. Atmeh AR, Chong EZ, Richard G, Boyde A, Festy F, Watson TF (2015) Calcium silicate cement-induced remineralisation of totallydemineralised dentine in comparison with glass ionomercement: tetracycline labelling and two-photon fluorescencemicroscopy. J Microsc 257:151–60. https://doi.org/10.1111/jmi.12197
42. Nakajima M, Sano H, Urabe I, Tagami J, Pashley DH (2000) Bond strengths of single-bottle dentin adhesives to caries-affected dentin. Oper Dent 25:2-10.
43. Erhardt MC, Toledano M, Osorio R, Pimenta LA (2008) Histomorphologic characterisation and bond strength evaluation of caries-affected dentin/resin interfaces: effects of long-term water exposure. Dent Mater 24(6):786-98. doi: 10.1016/j.dental.2007.09.007
44. Pashley DH, Tay FR, Yiu C, Hashimoto M, Breschi L, Carvalho RM, Ito S (2004) Collagen degradation by host-derived enzymes during aging. J Dent Res 83:216-21. doi: 10.1177/154405910408300306
45. Rahn BA, Perren SM (1971) Xylenol orange, a fluorochrome useful in polychrome sequential labelling of calcifying tissues. Stain Technology 46:125–9. https://doi.org/10.3109/10520297109067836
46. Atmeh AR, Chong EZ, Richard G, Festy F, Watson TF (2012) Dentin-cement interfacial interaction: Calcium silicates and polyalkenoates. J Dent Res 91:454-9. https://doi.org/10.1177/0022034512443068
47. Qi YP, Li N, Niu LN, Primus CM, Ling JQ, Pashley DH, Tay FR (2012) Remineralisation of artificial dentinal caries lesions by biomimetically modified mineral trioxide aggregate. Acta Biomater 8:836-42. doi: 10.1016/j.actbio.2011.10.033

Tables

Table 1: Description of materials used in the present study.

Group	Material	Commercial name	Composition	Manufacturer
control	Universal adhesive and flowable composite	ZipBond Aura	Adhesive: monomers including MDP, ethanol, water, fluoride Composite: Acrylic monomers as (6-46%), Diurethane dimethacrylate (6-46%), Triethylene glycol dimethacrylate (6-46%), 2,2-bis[4-(2-methacryloxy)ethoxy)phenyl] propane (6-46%)	SDI, Australia
GIC	Glass ionomer cement	Fuji IX	Powder: 95%w alumino-fluoro-silicate glass, 5% polyacrylic acid powder. Liquid: 50% distilled water, 40% polyacrylic acid, 10% polybasic carboxylic acid. Powder/liquid ratio: 3.6/1.0	GC, Japan
MTA	Trioxide mineral agreggate	Endo-Pass	Tricalciumsilicate, dicalciumsilicate, tricalciumaluminate, phyllosilicates (smectite and hydrotalcite), zirconium dioxide and barium sulfate	DEI Italia, Italy
RMTA	Resin-based trioxide mineral agreggate	TheraCal LC	Portland cement type III <60%, HEMA, polyethleneglycol dimethacrylate<50%, barium zirconate<10%	Bisco Inc, USA

FIGURES CAPTION

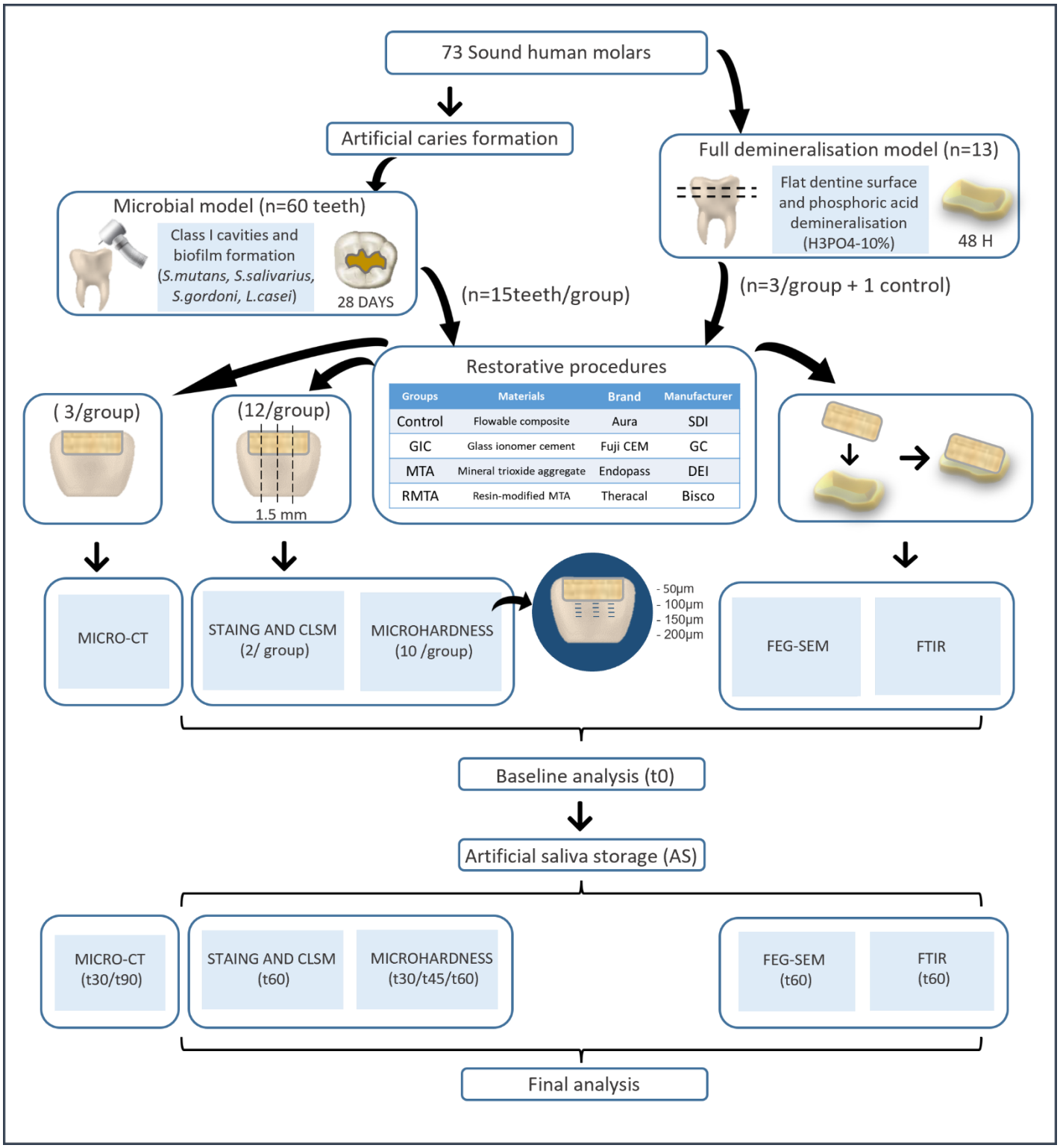

Figure 1: Distribution of specimens and methodological study design.

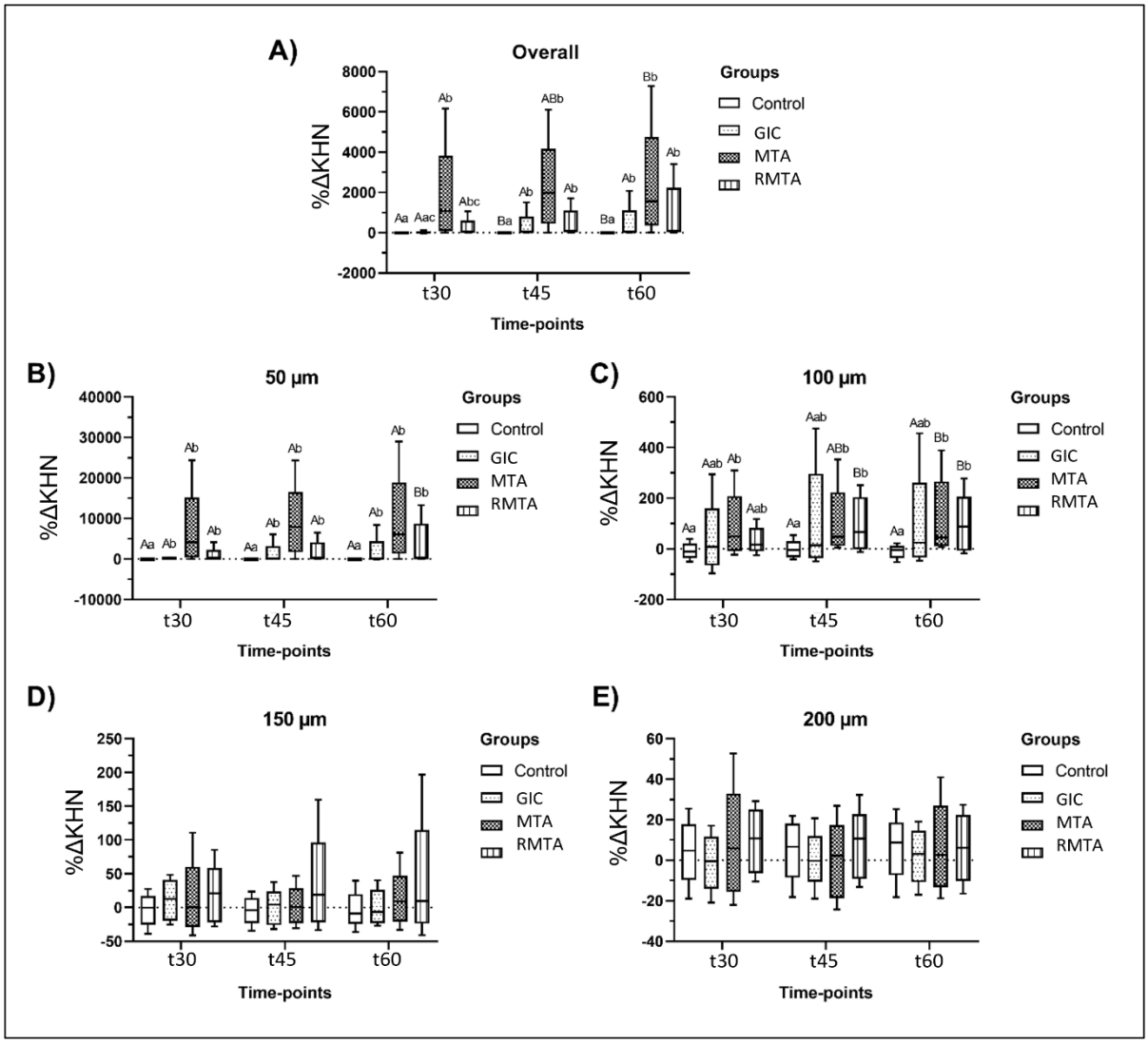

Figure 2: Microhardness assessment of tested materials at different depths and storage times. (A) Box plot of the overall microhardness (ΔKHN (%)) obtained at different time-points evaluation T1, T45, and T2 (average of the results of 50, 100, 150, and 200 µm). The ΔKHN (%) results obtained over time (T1, T45, and T2) at different depths are shown in figures (B) 50 µm, (C) 100 µm, (D) 150 µm, and (E) 200 µm.

Different uppercase letters indicate significant differences between the groups at different time-point evaluations (Friedman test; α=5%)

Different lowercase letters indicate a significant difference between groups at the same time-point evaluation (Kruskal-Wallis/Dunn tests; α=5%).

The absence of letters in graphs (D) and (E) indicates no differences between groups.

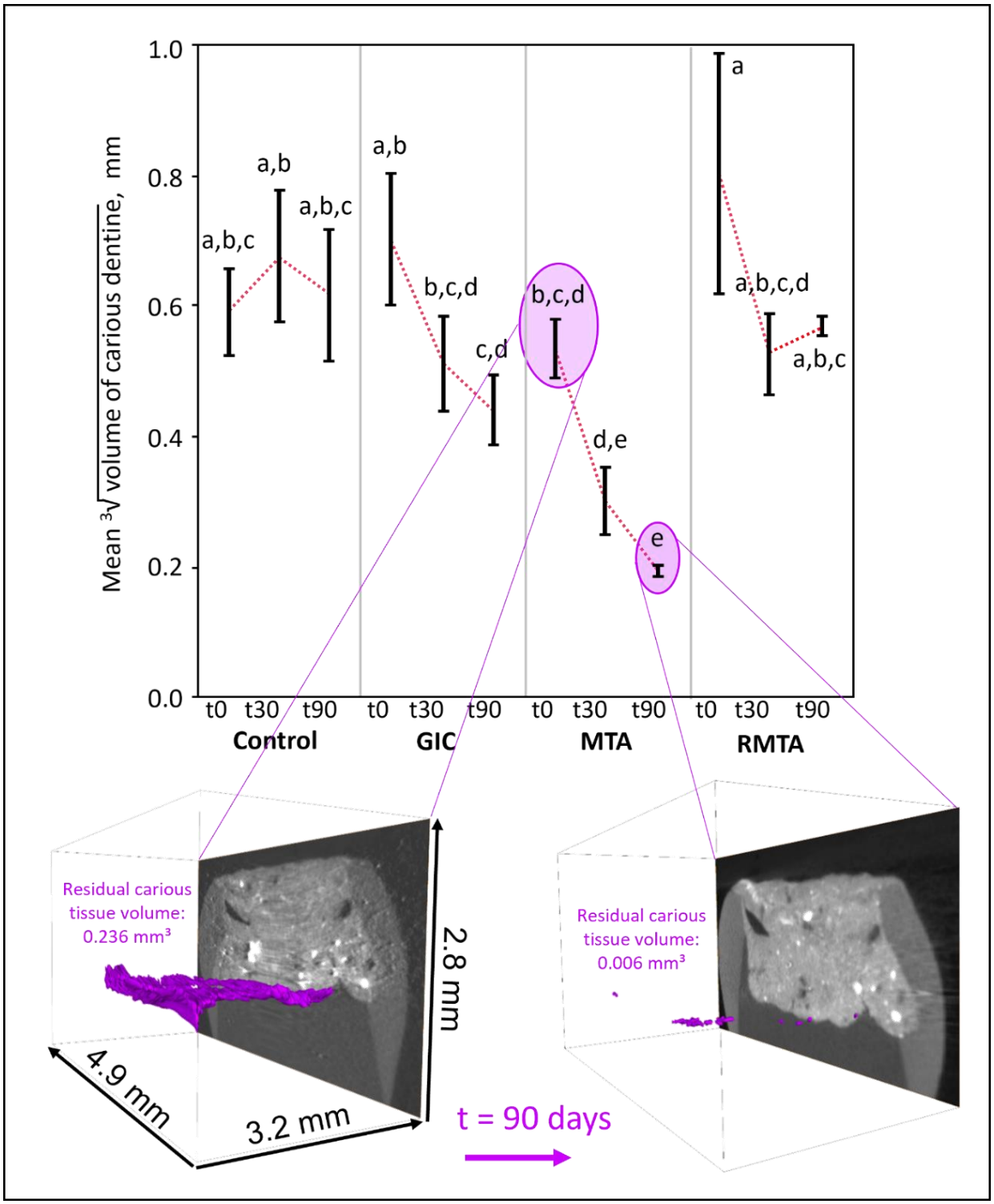

Figure 3: Micro-CT volumetric analysis of the carious dentine zone. Means and standard errors are indicated. Levels connected by different letters are statistically significant (Student's t-test; α=5%).

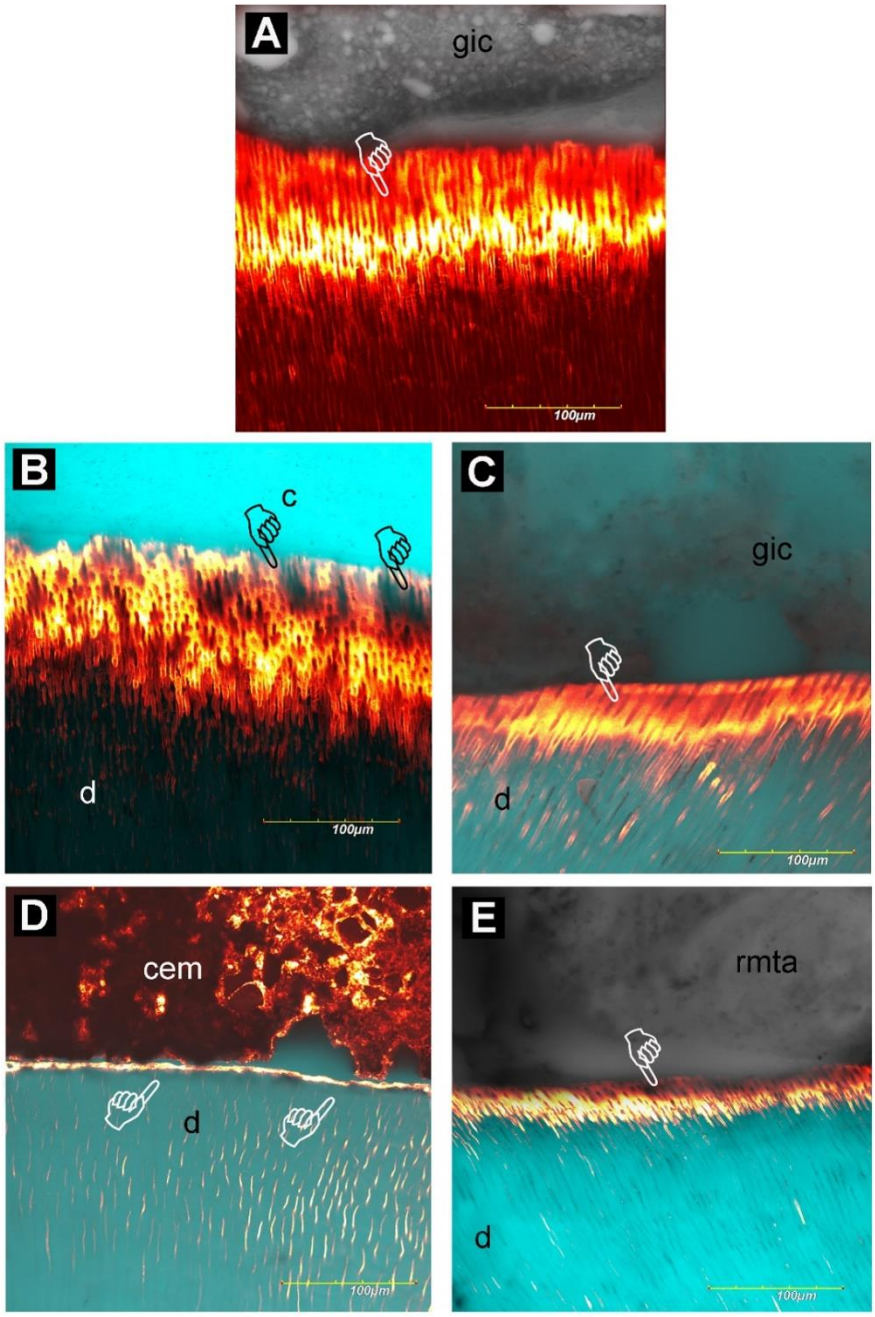

Figure 4: Confocal single projection images captured in transmission/fluorescence mode of the specimens treated with the different materials tested in this study and analysed after 60 d storage in AS. A) This is a comparative image in a specimen treated with the GIC at baseline (24h). An extended (100-120 µm) mineral-depleted dentine layer (pointer: simulated caries-affected dentine) just underneath the GIC-dentine (d) interface can be observed. Such a morphological scenario was comparable between all groups at the baseline. B) Adhesive+composite specimen showing no sign of remineralisation within the mineral-depleted dentine. Areas of degradation (pointers) occurred during the storage period. C) Morphological features observed in GIC-restored specimens. Most of the calcium-stained minerals accumulated only 30-40 µm underneath the GIC-dentine interface. D) MTA specimen showing residual calcium-stained minerals accumulated only few microns underneath the MTA-interface after prolonged storage in AS (pointer). Calcium-stained minerals are deposited also within the cement (cem). E) Specimen treated with RMTA. Similar to (D), calcium-stained minerals accumulated only few microns (pointer) underneath the RMTA-dentine (d) interface.

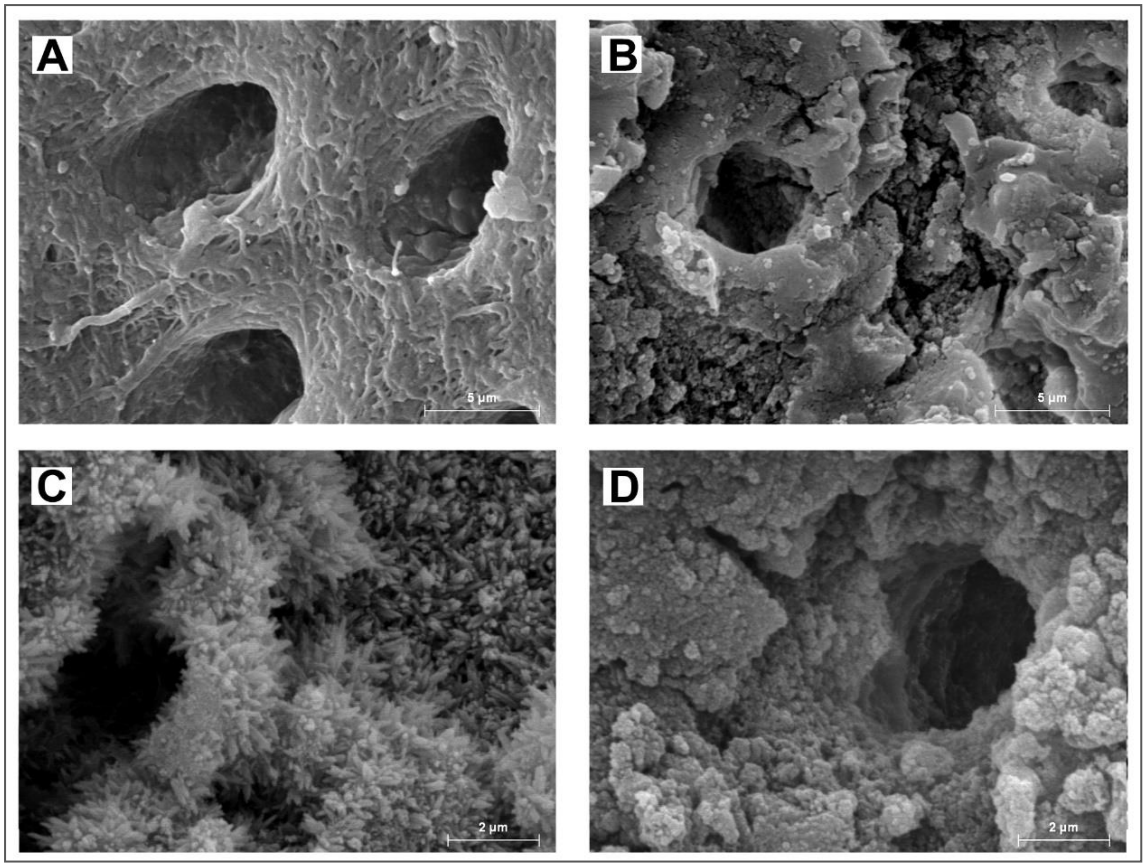

Figure 5: SEM micrographs obtained after prolonged storage (60 days) in AS. A) Representative specimen treated with conventional adhesive/composite materials showing the presence of demineralised dentine collagen fibrils with no presence of mineral precipitation (no signs of remineralisation). B) This specimen treated with GIC shows a surface with no exposed collagen fibrils, partially covered by minerals and residual material. C) This is a representative specimen treated with MTA where it is possible to note the clear presence of needle-like crystals deposited on the dentine surface. D) This specimen treated with RMTA presents globular-like crystals deposition of the dentine surface.

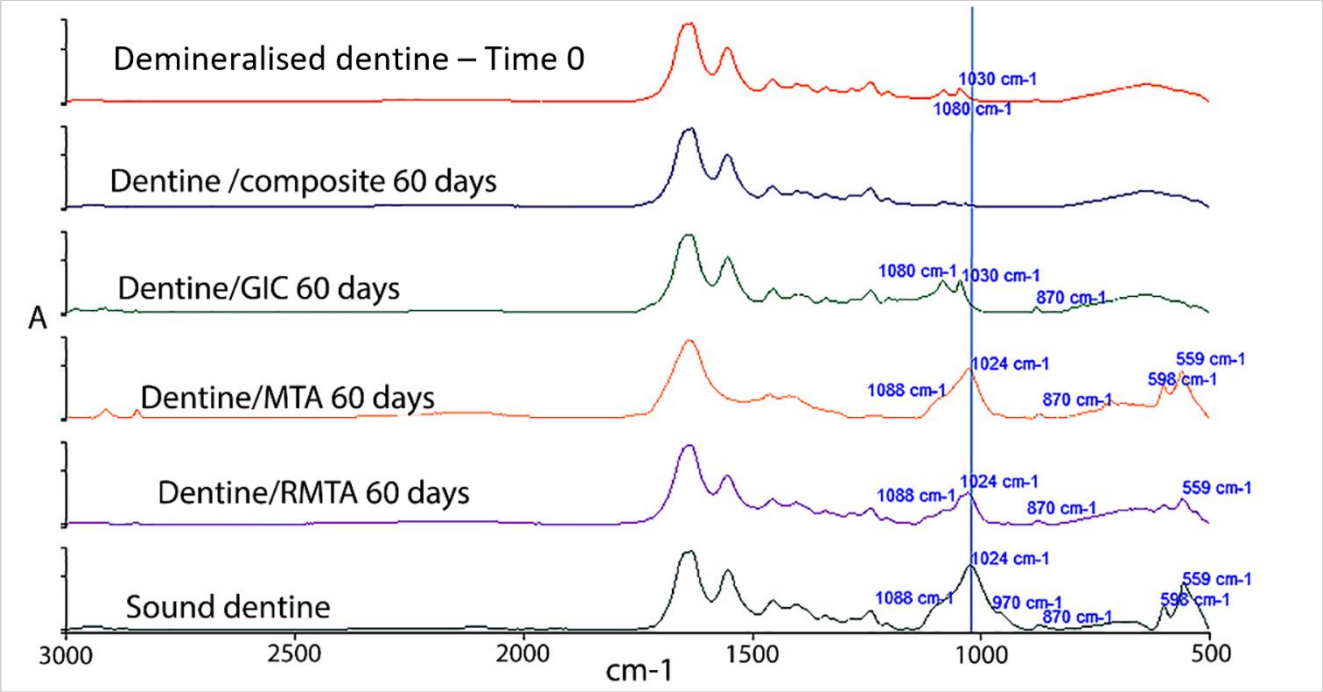

Figure 6: FTIR-ATR characterisation of demineralised dentine treated with the different tested materials and after 6 months storage in AS. The PO stretching of hydroxyapatite presents peaks at 559 cm^{-1}, 598 cm^{-1}, 970 cm^{-1}, 1024 cm^{-1} 1088 cm^{-1} and P–O(H) stretching at 870 cm^{-1}. The dentine collagen is visible at 1650 cm^{-1} (C O: amide I) and 1540 cm^{-1} (CNH: amide II).